Aquat. Sci. 65 (2003) 111–128
1015-1621/03/020111-18
DOI 10.1007/s00027-003-0645-x

Aquatic Sciences

Overview Article

Analysis of aquifer heterogeneity within a well capture zone, comparison of model data with field experiments: A case study from the river Wiese, Switzerland

Christian Regli [1,*], Martin Rauber [2] and Peter Huggenberger [1]

[1] Department of Earth Sciences, Applied and Environmental Geology, University of Basel, Bernoullistr. 16, 4056 Basel, Switzerland
[2] Rauber Consulting, Technoparkstr. 1, 8005 Zürich, Switzerland

Received: 16 December 2002; revised manuscript accepted: 21 March 2003

Abstract. This paper describes two groundwater models simulating a well capture zone in a heterogeneous aquifer located near an infiltrating river. A deterministic, large-scaled groundwater model (1.8 × 1.2 km) is used to simulate the average behavior of groundwater flow and advective transport. It is also used to assign the boundary conditions for a small-scaled groundwater model (550 × 400 m) which relies on stochastically generated aquifer properties based on site-specific drill core and georadar data. The small-scaled groundwater model is used to include the large subsurface heterogeneity at the location of interest. The stochastic approach in the small-scaled groundwater model does not lead to a clearly defined well capture zone, but to a plane representation of the probability of a certain surface location belonging to the well capture zone. The models were applied to a study site, which is located in an area of artificial groundwater recharge and production, in Lange Erlen near Basel, Northwestern Switzerland. The groundwater at this site contributes to the city's drinking water supply, and the site serves as a recreational area to the population of Basel. The river is channelized, but there are initiatives to restore the riverbank to more natural conditions. However, they conflict with the requirements of groundwater protection, especially during flood events. Therefore, a river section of 600 m in the vicinity of an unused and disconnected drinking water well was restored to study changes in the groundwater flow regime depending on hydrologic variations, water supply operation data, progress of river restoration, and subsurface heterogeneity. The results of the groundwater models are compared with data from two tracer experiments using Uranine and the natural Radon isotope Rn-222, and with physical, chemical, and microbiological data sampled in monitoring wells between the river and the drinking water well. The groundwater models document significant variations regarding the dimension of the well capture zone depending on changing boundary conditions and the variability of the hydraulic aquifer properties. The knowledge of the subsurface heterogeneity is important to evaluate transport times and distances of microorganisms from the infiltrating river or the riverbank to the drinking water well. The data from the monitoring wells show that chemical and microbiological processes predominantly occur in the hyporheic interstitial zone and the riverbank within a range of a few meters up to a few 10s of meters from the river. The methods presented here can be used to define and evaluate groundwater protection zones in heterogeneous aquifers associated with infiltration from rivers under changing boundary conditions, and under the uncertainty of subsurface heterogeneity. Furthermore, they allow one to study the site-specific operational alternatives associated with river restoration.

* Corresponding author phone: +41 61 267 3447;
fax: +41 61 267 2998; e-mail: christian.regli@unibas.ch
Published on Web: July 3, 2003

Key words. Well capture zone; hydrostratigraphy; geostatistics; sequential indicator simulation; groundwater modeling; river restoration; tracer; water quality.

Introduction

The fluvial deposits of river valleys are commonly important groundwater aquifers for municipal water supplies. In Switzerland, approximately 42% of the total drinking water demand, which is about 1.1 billion m^3/year, is covered by pumped groundwater. These groundwater aquifers are recharged by precipitation and river infiltration, but the relative contributions have not been examined in detail. Many of the river valleys are relatively narrow; so wells for water supply systems are commonly located near rivers.

In densely populated areas where public open space may be used as recreational areas as well as groundwater protection areas with activity restrictions, numerical methods for comparative assessment of different operational alternatives become a valuable tool. Groundwater models play an important role in decision-making processes (Reichert and Pahl, 1999), especially in the context of better characterization of parameter distributions and prediction of dynamic behavior of a given system. Groundwater models are helpful tools to define well capture zones based on hydrogeological and water supply operation data (e.g., Kinzelbach et al., 1992; Lerner, 1992). They allow one to study the sensitivity of the observed system with respect to changing parameters and conditions. However, groundwater models which do not consider site-specific geological information might not be acceptable for site-specific risk estimation of changing groundwater quality.

Vassolo et al. (1998), van Leeuwen et al. (1998), and others applied stochastic methods to cope with significant subsurface heterogeneity. The major advantage of the stochastic approach is its ability to account for uncertainty in the distribution of hydraulic aquifer parameters. In addition, stochastic methods can be used to check technical and operational measures on aquifers, to evaluate their effectiveness, or to evaluate measures for remediation of pollution (e.g., Rauber et al., 1998).

Model accuracy is strongly dependant on both the quantity and the quality of available data (Kinzelbach and Rausch, 1995). Data used in groundwater models may be divided into two basic types: “hard data” and “soft data” (Poeter and McKenna, 1995). Hard data (e.g., outcrop data, in some cases drill core data) can be directly obtained and examined. There is uncertainty in hard data, but it is considered small enough to be ignored. Soft data (e.g., georadar data) are less precise, thus greater uncertainties are associated with the soft data values. The problem of adequately modeling subsurface parameter distributions becomes more difficult with increasing heterogeneity and thereby increasing uncertainty with respect to the spatial variability of available data. The technique used to model subsurface structures in a site-specific problem should be chosen based on properties under consideration (e.g., lithofacies, hydraulic conductivity, porosity), available knowledge of the subsurface, and causes of uncertainty (Ayyub and Gupta, 1997; Weissmann et al., 1999). Considering these aspects, calculation, uncertainty estimation, and assessment of operational alternatives can be separated, the discussion in decision-making processes can be de-emotionalized, and discrepancies can be identified (Reichert and Pahl, 1999). A groundwater model based on geological data has accomplished its task, if the solution is robust, geologically and hydrologically reasonable, and if the actual parameter values differ only within a limited range from those of the model (Kinzelbach and Rausch, 1995).

Agricultural use of the floodplain, river corrections, and intensive hydroelectric power generation have deprived most Swiss perialpine rivers of their natural character. Excavation and the construction of dams and steps have resulted in deeper and narrower river channels with no connection to the adjacent floodplain. Therefore, these rivers often function primarily as conduits for precipitation runoff and overflow sewage, rather than as a natural aquatic biosphere. Different recent initiatives concentrate on restoring at least part of the original biodiversity of former floodplains. According to new legislation in Switzerland, the groundwater shall be protected by prevention of water pollution and implementation of well capture zones, and the ecological value of rivers shall be increased (Gewässerschutzgesetz, 1991). In many densely populated areas, these ideas lead to conflicting opinions about the best use of public open space.

The protection zones legally established are coupled with the licensed extraction volume of groundwater. Most of the existing protection zones legally delineated, however, are not based on the analysis of the dynamic character of the river-groundwater interaction nor on the influence of subsurface heterogeneity. The well capture zone is defined as the area from which about 90% of the maximum extracted groundwater originates, assuming a low groundwater table (Gewässerschutzverordnung, 1998). This definition is valid only for time-independent systems. For most groundwater systems, however, temporal dynamics should be considered, especially if a specific well capture zone is not the only one in the groundwater-bearing formation. In this case, different individual well capture zones mutually compete and influence each other. If the groundwater is polluted by chemicals or particles which are not sufficiently reduced or adsorbed (e.g., hormone effective and endocrine substances, gasoline additives, microorganisms), or if there is a danger of pollution by such substances, the delineation of well capture zones is of public interest (Gewässerschutzverordnung, 1998).

The main focus of this paper is to define and evaluate groundwater protection zones in heterogeneous aquifers associated with infiltration from rivers under changing boundary conditions, and under the uncertainty of subsurface heterogeneity. For such cases, methods presented here represent helpful tools for risk estimation of changing groundwater quality and quality management of water supplies, and for site-specific evaluation of operational alternatives for river restoration.

This paper starts with a description of the study site. Then deterministic and stochastic modeling of a well capture zone is presented depending on hydrologic variations, water supply operation data, progress of river restoration, and subsurface heterogeneity, including the generation of distributions of hydrogeological properties. This paper concludes with the comparison of results from groundwater models with two tracer experiments using Uranine and the natural Radon isotope, Rn-222, and also with physical, chemical, and microbiological data, sampled in monitoring wells between the river and the drinking water well.

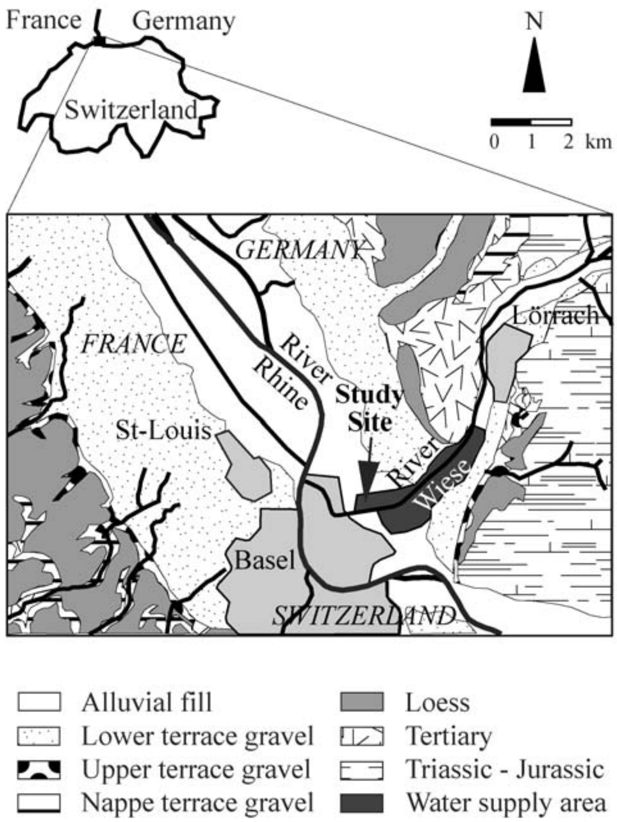

Figure 1. Simplified geological overview of Basel area in Northwestern Switzerland and location of study site – at the lower end of the city's water supply area Lange Erlen – within the ancient confluence of main river Rhine and its tributary Wiese.

Site description

The Lange Erlen serves as recreational area for the population of the city of Basel, as groundwater resource providing a significant portion of the city's drinking water (45'000 m^3/day). This water supply system extends over more than 4 km along the river Wiese as shown in Figure 1. The study site, at the lower end of the water supply area, is located in the ancient confluence of the main river Rhine (with flow to the Northwest) and its tributary Wiese (with flow to the Southwest).

The aquifer is artificially recharged with treated surface water (fast filtration) from the river Rhine. The water from the river Wiese or its artificial channels is not used to recharge the aquifer, because during the last 40 years its water was of poorer microbiological quality than Rhine water. Meanwhile, the chemical and microbiological water quality of the river Wiese has improved.

The unconfined aquifer consists of Quaternary unconsolidated coarse alluvial deposits. Tertiary marls underlie these gravels and are considered impermeable for the purposes of the model. The aquifer thickness varies between 13 and 18 meters. The lower 80% of the aquifer consists of Rhine gravel (primarily limestone) and the upper 20% of the aquifer consists of Wiese gravel (primarily silicates and limestone; Zechner et al., 1995). This may be explained by reworking of the Wiese gravel by the river Rhine under landscape-shaping conditions, whereby the top sequence of Wiese gravel will be preserved until the next shift of the active channel area of the river Rhine.

The average discharge of the river Rhine over the last 110 years is 1'052 m^3/s and is, therefore, around 90 times larger than the average discharge of the tributary Wiese with 11.4 m^3/s over the last 68 years (Bundesamt für Wasser und Geologie, 2001). The river Wiese has been channelized during the last century. Two dams at distances of 55–60 m protect the adjacent plain from flooding. The cross-section is double trapeziform, the actual river width is 20 m. Elevation change in the riverbed is achieved with incremental step heights of about 0.1 m, and the average slope is about 4.5‰.

The riverbed mobilizes during floods. It was observed that an increase of the infiltration of river water into groundwater pollutes drinking water wells located near the rivers, especially during flood events. Therefore, river restoration conflicts with the safety requirements of the groundwater protection zones.

The riverbed within the study site has been restored because of its function as a recreational area. The restored section consists of two parts with a total length of ap-

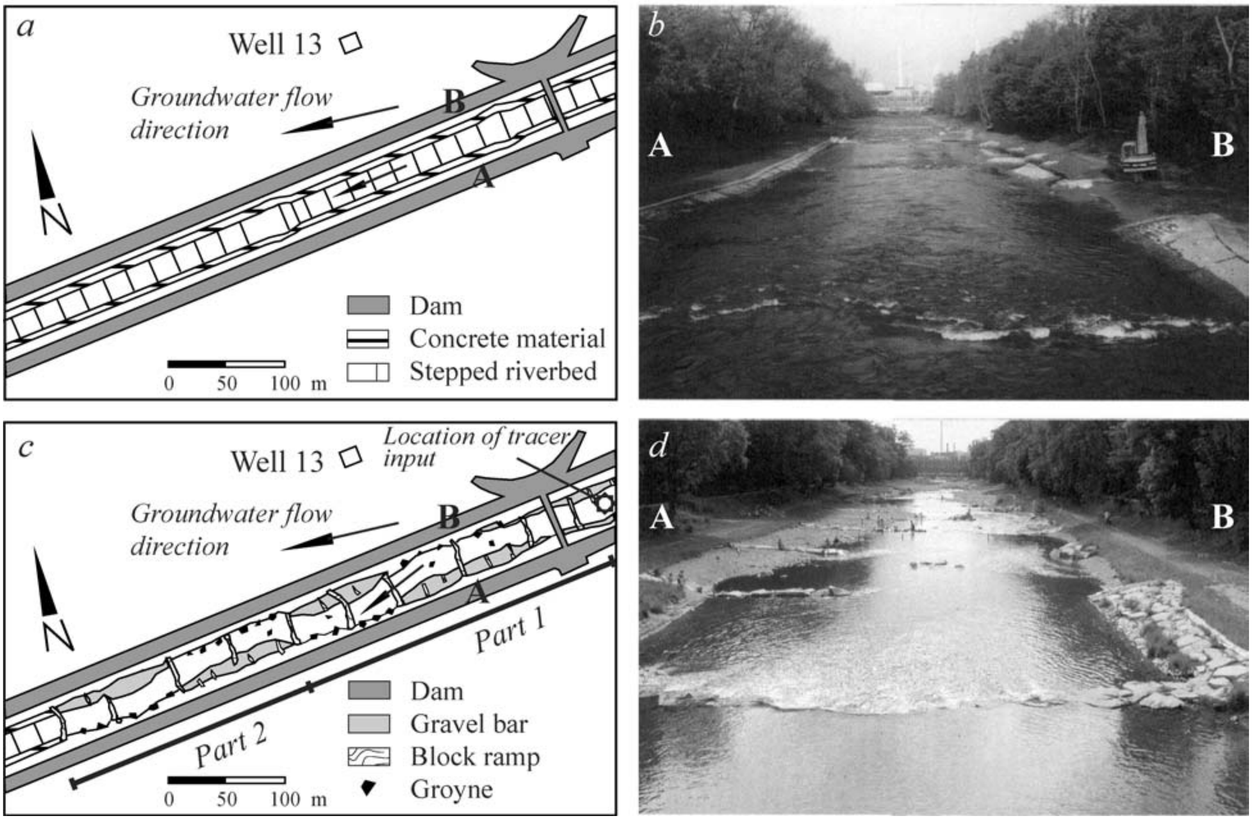

Figure 2. Part of the river Wiese before and after restoration operation: (a) plan view and (b) photo of straightened and artificially stepped river; (c) plan view and (d) photo of restored river with improved lengthwise and crosswise connectivity through the replacement of steps with block ramps and concrete material with gravelled riparian zones. In the photos, the flood protection dams are located within the woods.

proximately 600 m and includes 10 block ramps, 28 groynes, and 4 gravel bars. The weight of the built-in rock blocks was 3'180 tons; however, the volume of these blocks is smaller than that of the concrete material removed. Gravel was only redistributed, and no additional gravel material was supplied. Figure 2 shows the river Wiese before and after restoration operation. The restoration in part 2 is far enough downstream that it has no influence on any well capture zone.

For groundwater monitoring, 11 new boreholes were drilled along hypothetical groundwater flow paths between the river Wiese and drinking water well 13, which is located at a distance of about 120 m from the river and is no longer used for water supply. Nine of the new boreholes are grouped in clusters of three boreholes each as shown in Figure 3. The boreholes have been drilled to specified aquifer depths. Monitoring wells 1458, 1472, 1473, and 1475 sample the aquifer about 1–2 m below the average groundwater table; monitoring wells 1459, 1461, 1462, and 1476 sample the middle part of the aquifer; and monitoring wells 1460, 1474, and 1477 sample the aquifer a few meters above the relatively impermeable Tertiary marls. Five drill cores covering the whole aquifer thickness have been described sedimentologically. These cores were used to calibrate the 14 vertical georadar reflection sections which were recorded in the vicinity of drinking water well 13 to characterize the subsurface heterogeneity.

The question of whether and how river restoration might negatively affect groundwater quality were the objects of an accompanying investigation program. The field experiments as well as the regular and flood-event specific measurements are shown in Table 1.

Aquifer and groundwater modeling

Groundwater flow and coupled advective transport were simulated with two different models using Processing Modflow (PMWIN) from Chiang and Kinzelbach (2001). Figure 4 shows the situation. The following sub-section describes the deterministic, large-scaled groundwater model which was used to simulate average groundwater flow and advective transport and allows one to define boundary conditions for telescoped model areas. Then, the small-scaled groundwater model is described which relies on stochastically generated aquifer properties based on site-specific drill core and georadar data.

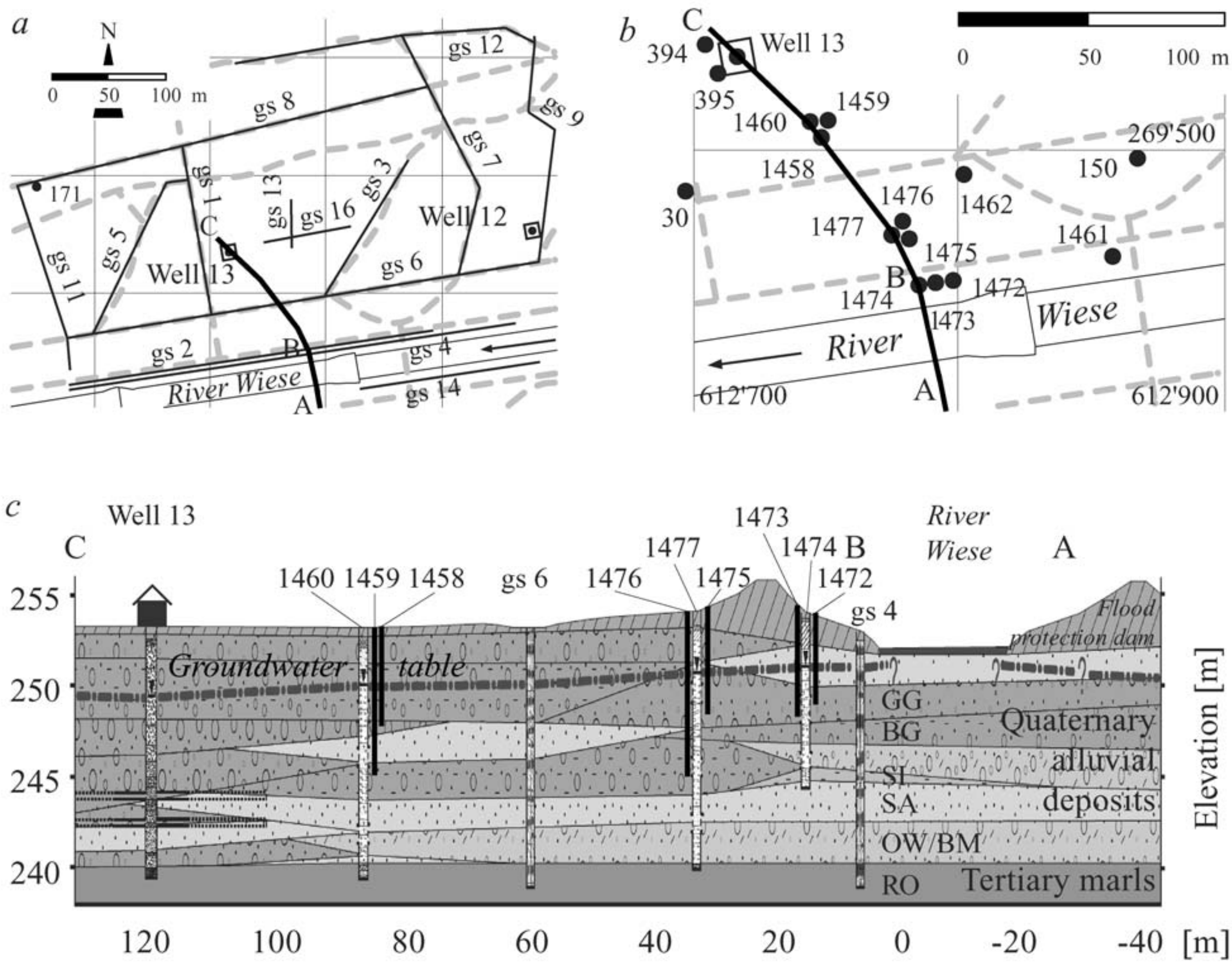

Figure 3. Plan view of study site and vertical geological section: (a) traces of georadar sections (gs) and drinking water wells; (b) monitoring wells, partially grouped in clusters, sampling the upper, middle, and lower part of the aquifer; (c) vertical geological section (vertically enlarged by a factor of 3) along monitoring wells showing the subsurface heterogeneity within the capture zone of drinking water well 13.

Table 1. Investigation program accompanying the river restoration within the capture zone of drinking water well 13.

Investigation program	Before river restoration		After river restoration	
	regularly sampling (weekly)	event-specific sampling (daily)	regularly sampling (weekly)	event-specific sampling (daily)
Artificial tracer experiment: *Uranine*		*X*		*X*
Natural tracer experiment: *Radon-222*				*X*
Physical and chemical measurements: *DOC, O2, pH, Ca, HCO3, Temperature, Electrical conductivity, NH4, NO2, NO3, PO4, SO4, Cl, Turbidity*	*X*	*X*	*X*	*X*
Microbiological measurements: *Heterotrophic plate counts, Escherichia coli, Enterococcus*	*X*	*X*	*X*	*X*

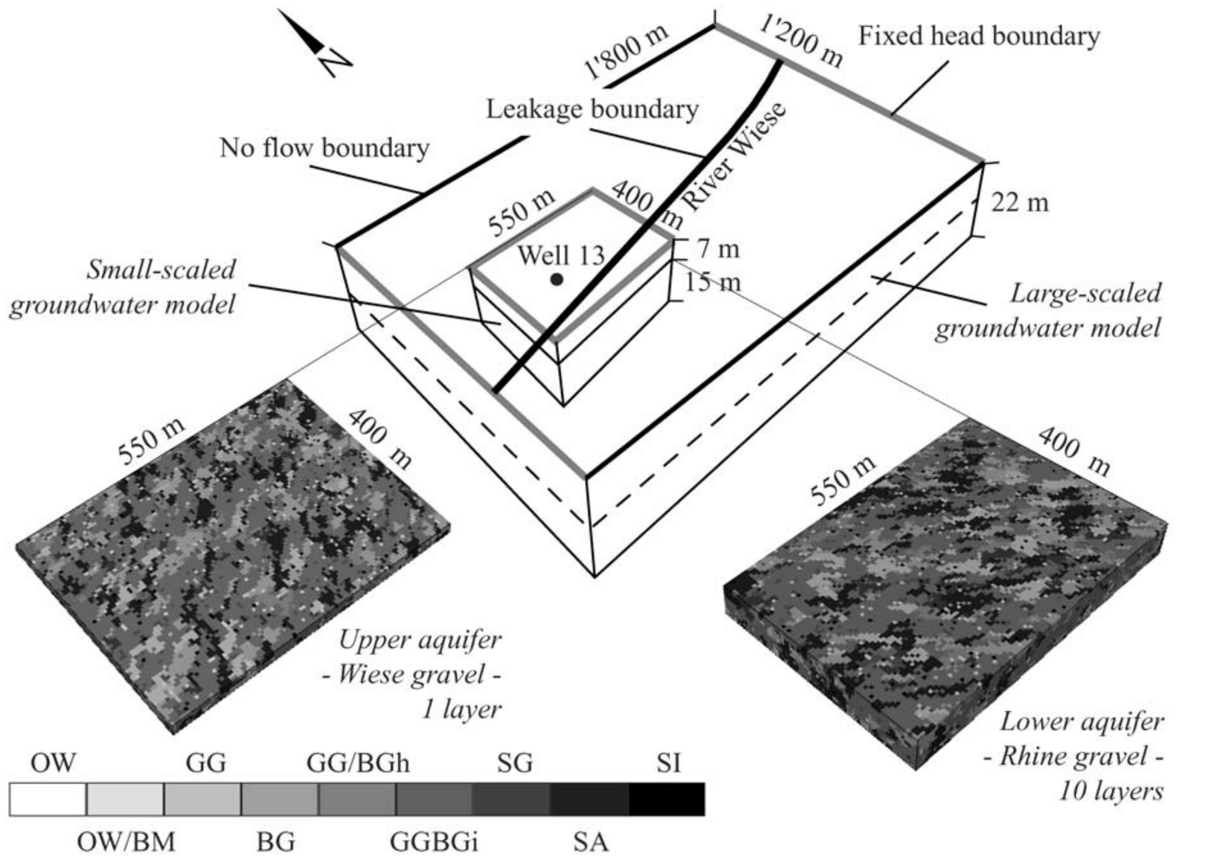

Figure 4. Situation of the large-scaled, homogeneous groundwater model and the small-scaled groundwater model, which relies on stochastically generated aquifer properties. OW: open-framework gravel, OW/BM: open-framework/bimodal gravel couplets, GG: gray gravel, BG: brown gravel, GG/BG-horizontal: alternating gray and brown gravel, horizontally layered, GG/BG-inclined: alternating gray and brown gravel, inclined, SG: silty gravel, SA: sand, SI: silt.

Calibration and results of the large-scaled groundwater model

The large-scaled, two-layer finite-difference groundwater model has a total of 39'032 cells and covers an area of 1'800 × 1'200 m. The cell size varies from 5 × 5 m, within the zone of river restoration, to 20 × 20 m. The model is divided in two layers having a thickness of approximately 4–8 m and homogeneous hydraulic parameters. Model boundary conditions are of the first type (fixed head boundary) along the Eastern and Western side, and of the third type (leakage boundary) along the river Wiese. The Northern and Southern sides are specified as no flow boundaries. The topography of the aquifer bottom (Tertiary marls) is interpolated from the top levels of the bedrock. The available data are based on the drill core descriptions and georadar recordings.

The data-sensitive parameters of the steady-state, large-scaled groundwater model – the hydraulic conductivity of the two model layers and the leakage factor (Chiang and Kinzelbach, 2001) of the riverbed – are calibrated with data from December 9, 1998. The data are based on 69 groundwater head measurements, 4 river stages, and corresponding pumping and recharge rates. Solutions of the groundwater flow equation match the field head data with a mean squared deviation of 0.14 m^2. The calibrated hydraulic conductivity is 5.75 E-3 m/s for both the upper and lower layer. The leakage factor of the river Wiese is 1 E-6 /s.

Figure 5 shows simulations of the capture zone of drinking water well 13 that was approximately determined by particle tracking for conditions before and after river restoration as well as for low river discharge, and moderate and high floods. Figure 5a represents the calibrated groundwater model. In Figure 5b–f predictions under changed boundary conditions are given. The well capture zone is strongly influenced by changing river discharge and the structure of the riverbed. River restoration is simulated by increasing the leakage factor by a factor of 10 and 100, respectively, within the restored river channel, assuming moderate and strong increase of the hydraulic conductivity of the riverbed. The leakage factor of the artificially built gravel bars was not increased. The modeled infiltration of river water within the well capture zone varies between < 0.02 $m^3/m^2/d$ (Fig. 5a) and

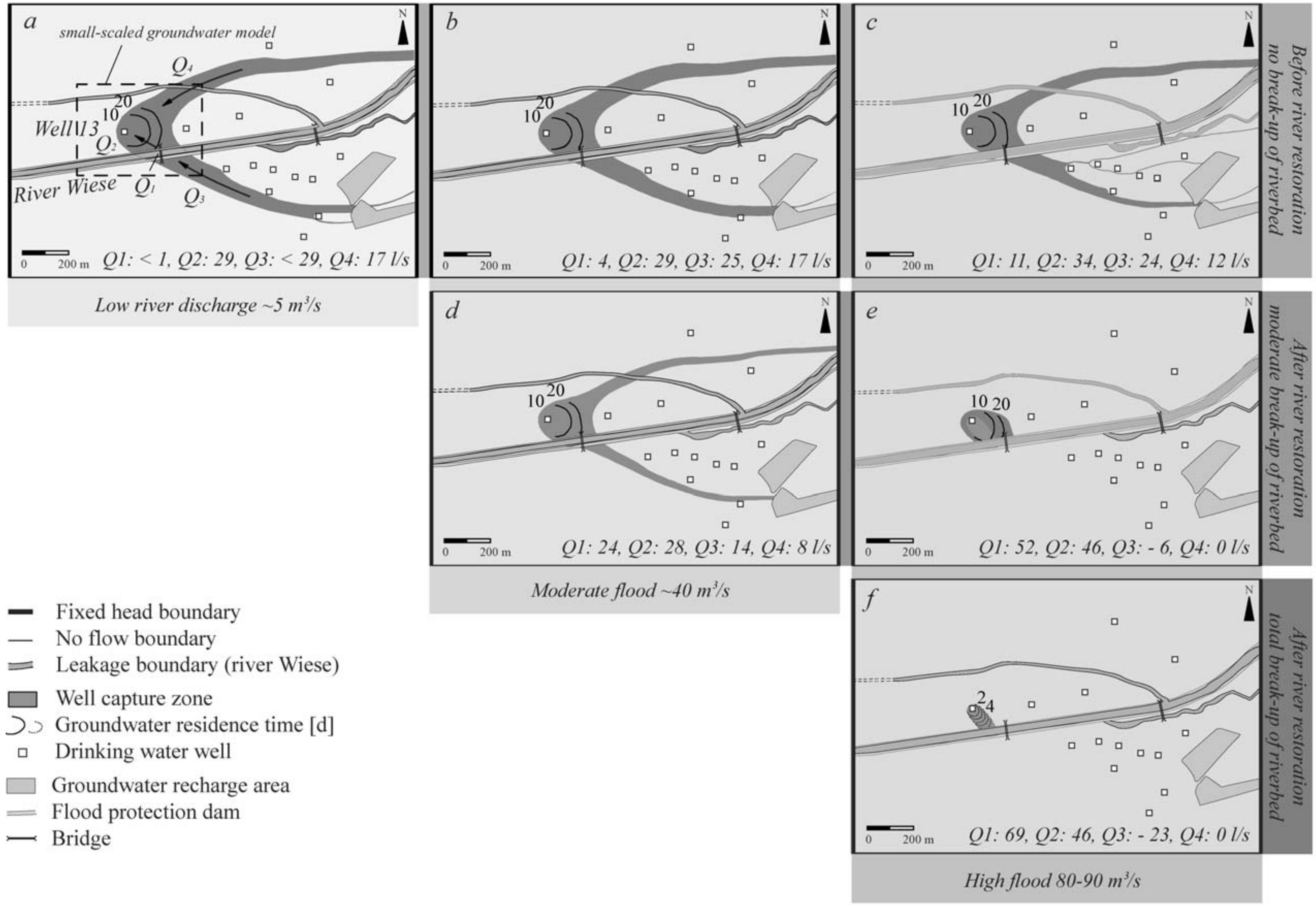

Figure 5. Changes of the capture zone of drinking water well 13 in the large-scaled groundwater model depending on river discharge, river restoration, and water supply operation data: (a–c) before river restoration; (d–f) after river restoration (increasing the leakage factor by a factor of 10 (d,e) and 100 (f)); (a) low river discharge (~5 m^3/s); (b,d) moderate flood (~40 m^3/s); (c, e, f) high flood (80–90 m^3/s). The groundwater extraction at drinking water well 13 is constant at 0.046 m^3/s. Water budgets within the well capture zone [l/s]: Q1: river leakage, Q2: horizontal groundwater flow (right side of river Wiese), Q3: horizontal groundwater flow (left side of river Wiese), Q4: horizontal groundwater flow (North-eastern of drinking water well 13).

> 3.06 $m^3/m^2/d$ (Fig. 5 f). Particularly at high flood events, the model results show a short travel time between the riverbed and the drinking water well 13.

Based on the large-scaled, homogeneous model results, the average groundwater residence time between the river Wiese and drinking water well 13 varies between 20 (Fig. 5 a) and 5 days (Fig. 5 f). In general, it is expected that in restored rivers, mobilization of the riverbed does not occur at the same time nor to the same extent as before river restoration. Therefore, particularly during flood events, the permeability of the riverbed will vary considerably because of both the higher discharge dynamics in restored rivers compared to channelized rivers and the temporal variability of zones with higher infiltration.

Generation of aquifer properties and results of the small-scaled groundwater model

At Basel about 3000 drill-core descriptions from Basel are stored in a data base (Noack, 1993; Noack, 1997). This is a comprehensive source of information for site characterizations. For the generation of aquifer properties at the small scale, a combined sedimentological and geostatistical approach was chosen. The sedimentological approach is based on observations in unweathered outcrops and fluvio-dynamic interpretations of processes in a braided river system (Siegenthaler and Huggenberger, 1993; Jussel et al., 1994) and allows a lithofacies-based interpretation of drill core and georadar data to provide conditioning data for the stochastic aquifer simulation (Regli et al., 2002). The geostatistical approach matches the sedimentary structures based on the conditioning data and the spatial correlation of the data values (e.g., Deutsch and Journel, 1998). The aquifer properties are then integrated into the small-scaled groundwater model for steady-state flow and coupled advective transport simulation. Observed groundwater heads are used to restrict the choice of aquifer realizations to those yielding acceptable simulated groundwater heads at the observation points.

Sedimentological and geophysical analysis of the Rhine/Wiese aquifer. As noted above the lithology of the Rhine and Wiese sediments is easily distinguished because the sediments are from different source areas which have distinct geological units. Within these two stratigraphic units a number of sedimentary structures are recognized that were generated by sedimentary processes in the braided fluvial system. Lithofacies associated with the sedimentary structures at this location include (Regli et al., 2002): open-framework gravel (OW), open-framework/bimodal gravel couplets (OW/BM), gray gravel (GG), brown gravel (BG), alternating gray and brown gravel layers (GG/BG), horizontally layered or inclined, silty gravel (SG), sand lenses (SA), and silt lenses (SI). The principal relationship of the lithofacies types and the sedimentary processes which form these structure types are described in Siegenthaler and Huggenberger (1993).

The boreholes and georadar investigations (Fig. 3) were made to delineate the main sedimentary structures as described above. The total length of the georadar sections is 3'040 m. The three-step method presented in Regli et al. (2002) was used to interpret the sedimentological and geophysical data. In the first step, the site-specific lithofacies scheme to classify sedimentary structure types is established based on outcrop data. In the second step, the probability that a drill core layer description represents a certain sedimentary structure type is estimated. In the last step, drill core layers and corresponding radarfacies types are related.

This lithofacies-based interpretation of drill core and georadar data respects differences in data uncertainty and provides structure-type probabilities for points along boreholes and for grid nodes with arbitrary mesh sizes along georadar sections. The sampled data from the georadar sections at this location are given for grid nodes separated by 5 × 1 m.

Stochastic generation of aquifer properties. GEOSSAV (Geostatistical Environment fOr Subsurface Simulation And Visualization) is a tool for the integration of hard and soft data into the 3D stochastic simulation and visualization of distributions of geological structures and hydrogeological properties in the subsurface (Regli et al., submitted). GEOSSAV was used to generate the sedimentary structures and the hydraulic aquifer properties in the vicinity of drinking water well 13, which are integrated into the small-scaled (550 × 400 × 22 m), 11-layer finite-difference groundwater flow and advective transport model. GEOSSAV, as an interface to selected geostatistical programs from the Geostatistical Software LIBrary, GSLIB (Deutsch and Journel, 1998), can be used for data analysis, variogram computation of regularly or irregularly spaced data, and sequential indicator simulation of subsurface heterogeneities. The simulations can be visualized by 3D rendering and slicing perpendicular to the main coordinate axis. The data can be exported into regular grid-based groundwater simulation systems (e.g., GMS (Environmental Modeling Systems Inc., 2002); PMWIN (Chiang and Kinzelbach, 2001)).

The variogram computation is based on the drill core and georadar data described above. The variography was run separately for the lower part (Rhine gravel) and the upper part (Wiese gravel) of the aquifer. The indicator transform (Deutsch and Journel, 1998) at grid node locations is set to 1 for the structure types with the greatest probability values, or is set to 0 otherwise. Experimental indicator variograms are calculated for various directions (azimuth, dip, plunge). The resulting variogram information for the nine sedimentary structure types identified

Table 2. Variogram information of Rhine and Wiese gravel used for the sequential indicator simulation to define the geometric anisotropy of the sedimentary structure types: OW: open-framework gravel, OW/BM: open-framework/bimodal gravel couplets, GG: gray gravel, BG: brown gravel, GG/BG-horizontal: alternating gray and brown gravel, horizontally layered, GG/BG-inclined: alternating gray and brown gravel, inclined, SG: silty gravel, SA: sand, SI: silt. The values written in italics are estimates; the isotropic nugget constant of the sedimentary structure types are 0; the variogram models of the sedimentary structure types are exponential; the dip and plunge of the sedimentary structures are 0.

	Sedimentary structure type Variogram parameter	OW	OW/BM	GG	BG	GG/BG horizontal	GG/BG inclined	SG	SA	SI
Wiese gravel	Probability density function	*0.02*	0.05	0.16	0.05	*0.50*	*0.05*	0.02	0.14	*0.01*
	Sill	*0.13*	0.12	0.18	0.115	*0.13*	*0.13*	0.045	0.18	*0.13*
	Azimuth [°]	*240*	240	240	240	*240*	*240*	270	200	*240*
	Max. horiz. range [m]	*3*	24	60	34	*50*	*7*	14	50	*3*
	Min. horiz. range [m]	*1.5*	18	24	24	*18*	*3*	18	16	*1.5*
	Vertical range [m]	*0.5*	4	6	5	*6*	*1*	4	3	*0.5*
Rhine gravel	Probability density function	*0.02*	0.06	0.12	0.05	*0.50*	*0.05*	0.03	0.16	*0.01*
	Sill	*0.1*	0.095	0.155	0.055	*0.1*	*0.1*	0.04	0.17	*0.1*
	Azimuth [°]	*310*	320	315	300	*310*	*310*	300	300	*310*
	Max. horiz. range [m]	*5*	54	60	40	*70*	*8*	30	60	*5*
	Min. horiz. range [m]	*2*	22	19	22	*30*	*4*	17	22	*2*
	Vertical range [m]	*1*	10	5	11	*10*	*2*	10	8	*1*

in the study site is given in Table 2. Azimuth, dip, plunge, and the ranges corresponding to maximum and minimum horizontal and vertical distances of spatial correlation characterize the geometric anisotropy of the sedimentary structure types (Deutsch and Journel, 1998). The initial probability density functions (Deutsch and Journel, 1998) are based on the data density representing a specific structure type. The values written in italics are estimated because the corresponding structure types never have the greatest probabilities and, thus, the indicator transform always would be set to 0 by default for these structure types.

The main outcome of the variogram analysis is the orientation of the sedimentary structure types representing the main flow direction of the river Rhine in the lower part of the aquifer and the tributary Wiese in the upper part of the aquifer. The relatively large ranges of spatial correlation of a few meters up to a few 10s of meters for the different sedimentary structure types (Table 2) may be significantly influenced by the resolution of the georadar system and the density of the sampled data taken from the georadar sections. The sedimentary structures of the Rhine gravel are modeled as geostatistical structures that are horizontally around 20% and vertically around 45% larger than the structures of the Wiese gravel.

The aquifer is simulated by sequential indicator simulation (Deutsch and Journel, 1998). The sequential indicator simulation principle allows conditioning by including all data available within the neighbourhood of a model cell, including the original data and all previously simulated values. The steps in the sequential indicator simulation are as follows: In the first step, a grid network and coordinate system is established. In the second step, the existing data is assigned to the nearest grid node. If there is multiple data available, only the closest data is assigned to the nearest grid node. In the third step, a random path through all grid nodes is determined. For a node in the random path: (1) the nearby data and previously simulated grid nodes are searched, and (2) the conditional distribution is estimated by indicator kriging (Deutsch and Journel, 1998). From this distribution (3) a simulated lithofacies is randomly drawn and set as hard data. Then the next node in the random path is selected and the steps (1)–(3) are repeated. This way, the simulation grid is built up sequentially. In the last step, the results are checked. The data and the global proportions (random function hypothesis: limited deviations of the input and output probability density functions of the sedimentary structure types) have to be honored, and the orientations and sizes of the sedimentary structures have to be in accordance with the observed sedimentary structures.

In Figure 4 one realization of the sequential indicator simulation is shown with separate realizations for the lower and the upper parts of the aquifer. The regular model grid of the lower part is defined by $110 \times 80 \times 10$ cells and of the upper part by $110 \times 80 \times 1$ cells. The cell sizes of the lower part are $5 \times 5 \times 1.5$ m and of the upper part $5 \times 5 \times 7$ m. However, the saturated thickness of the topmost layer is about 1–2 m.

A total of ten combinations of sedimentary structure-type distributions were simulated, each called an aquifer realization. The resulting probability density functions of the sedimentary structure types deviate less than $\pm 10\%$ from the initial probability density functions. For determining statistical moments and their confidence limits by a Monte Carlo type modeling more than 100 or 1000 realizations are needed. However, to qualitatively examine the effects of subsurface heterogeneity in this boundary condition dominated model (changes in river discharge and permeability of riverbed), a smaller number of aquifer realizations already produces the main trends of groundwater flow and transport behavior.

The changes in orientation and ranges of the sedimentary structures, caused by the above-mentioned interactions of the two rivers over time, are recognized and included in the model by partitioning the aquifer vertically into two hydrostratigraphic units. The generated sedimentary structures are characterized by randomly selecting hydraulic conductivity and porosity values given by means and variances in Jussel et al. (1994) and Rauber et al. (1998). Then, files with the distributions of the hydraulic parameters are generated and exported into PMWIN (Chiang and Kinzelbach, 2001) to perform steady-state groundwater flow and transport simulations.

Results of the small-scaled groundwater model. For each aquifer realization, a flow model computation was performed and the capture zone for drinking water well 13 was approximately defined by particle tracking. By superposition of all capture zones produced, a probability distribution is obtained that describes the probability of a certain surface location belonging to the capture zone. This probability is given by the fraction of capture zones among all realizations containing the location.

Figure 6 shows probability distributions of the capture zone of drinking water well 13 for conditions before and after river restoration as well as for low river discharge, moderate and high floods. Figure 6a represents the calibrated groundwater model. The average of the mean squared deviations of observed versus calculated heads over the 10 flow simulations is 0.10 m^2. In Figure 6b–f, predictions under changed boundary conditions are given, with each probability distribution representing the result of 10 flow and advective transport simulations.

The probability distribution of the well capture zone is strongly influenced not only by changing river discharge and riverbed structure, but also by subsurface heterogeneity. Preferential flow paths can be detected to some extent. In particular, zones along the riverbank with increased infiltration rates of river water can be recognized. River restoration is simulated by increasing the leakage factor by a factor of 10 and 100, respectively, within the restored river channel, assuming moderate and strong increase of the hydraulic conductivity of the riverbed. The leakage factor of the artificially built gravel bars was not increased.

The small-scaled groundwater model produces probable well capture zones depending on the uncertainty of the available data representing sedimentary structure types and the variability of hydraulic conductivity and porosity values for each. The groundwater residence times vary between 1 and 20 days.

Comparison of model results with field data

Tracer experiments

A first tracer experiment with Uranine was run before river restoration (March 9 – July 3, 1998) during a moderate flood event to determine the stretch of riverbed which should be restored such that no upstream well capture zone would be influenced. The results are also used to determine the sampling frequency for event-specific physical, chemical, and microbiological measurements. The tracer was released into the groundwater between the river Wiese and the right main flood protection dam. The tracer experiment is described in Huggenberger and Regli (1998).

A second tracer experiment with Uranine was run after river restoration (December 13–30, 1999) during a moderate flood event to determine the river-groundwater interaction and groundwater residence times between the river Wiese and drinking water well 13. The tracer was released into the river slightly upstream of the restored river section. Uranine has a retardation factor in sandy gravel of 1.2 and its detection limit is 0.002 ppb (Schudel et al., 2002). To enhance the lateral mixing of the tracer in the river, 10 kg Uranine dissolved in 40 liters of water was evenly distributed over the entire cross-section of the river. The river discharge averaged 39.6 m^3/s during the Uranine release. The groundwater extraction rate at drinking water well 13 was constant at 0.046 m^3/s.

The breakthrough curves at monitoring wells 1461, 1472, 1474, 1475, 1476, 1477, 30, 1459, and 1460 (grouped according to distance from the river) are shown in Figure 7a–c. They document a relatively slow vertical mixing of the aquifer. The breakthrough of the tracer is delayed and has a decreased peak concentration with increasing depth. The breakthrough curve of monitoring well 1477 is influenced by the second flood event from December 18 to 21, which followed the first flood event on December 13, 1999. The breakthrough of wells 1475 and 1476 in the upper part of the aquifer occurred before the second flood event.

The breakthrough curve at drinking water well 13 (Fig. 7d) shows minimum (approximate), dominant, average, and maximum (approximate) groundwater residence times of 28 h (1.2 d), 103 h (4.3 d), 123 h (5.1 d), and 400 h (16.7 d), respectively. These residence times indicate the existence of fast flow paths as predicted by simulations of the small-scaled groundwater model. The maximum tracer concentration in drinking water well 13 was 0.04 ppb and the dilution rate was 1 : 3’500. The recovery of 1.2 g of the tracer in drinking water well 13 documents infiltration of river water within the well capture

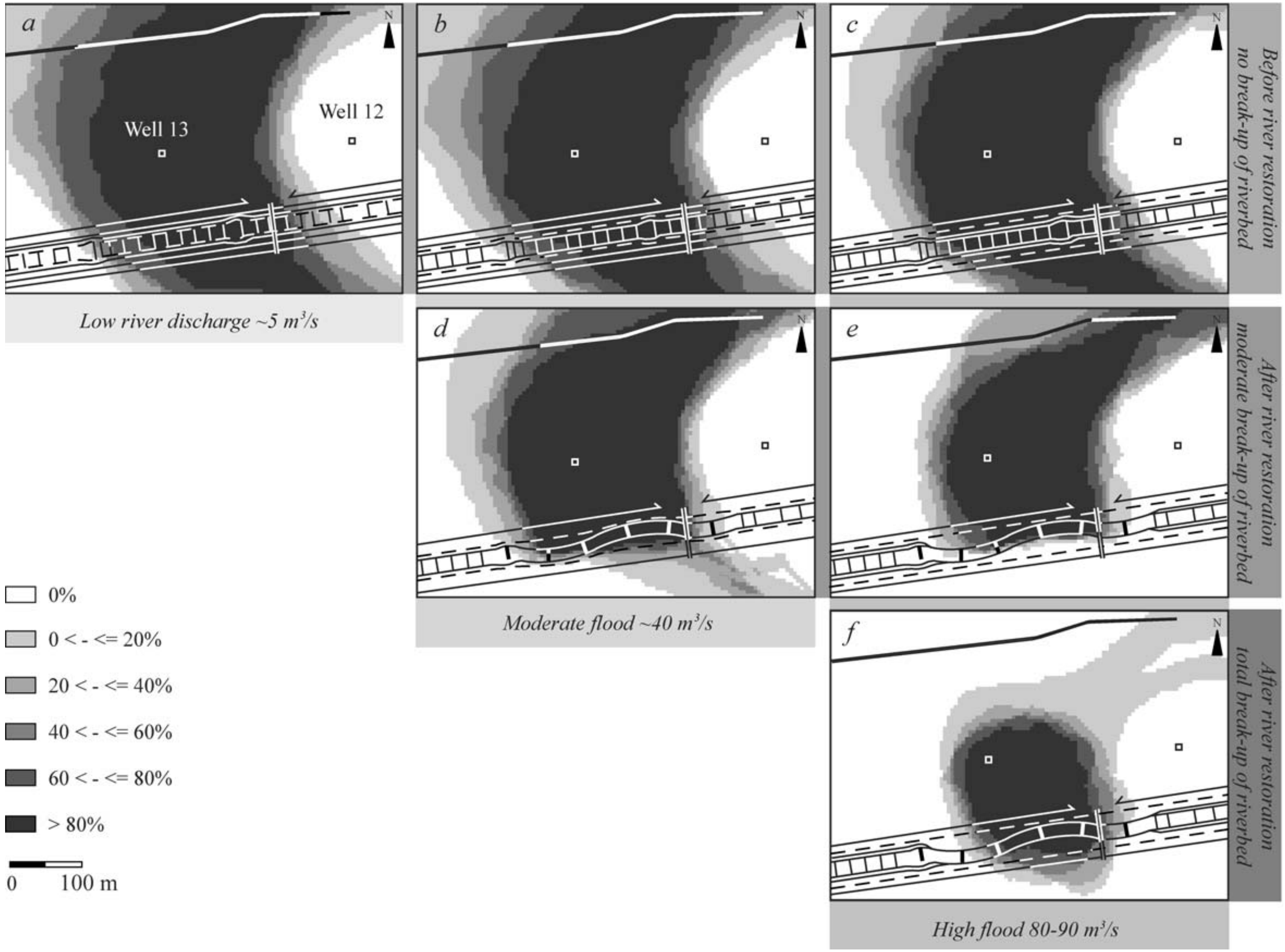

Figure 6. Changes of the capture zone distribution of drinking water well 13 in the small-scaled groundwater model depending on river discharge, river restoration, water supply operation data, and subsurface heterogeneity: (a–c) before river restoration; (d–f) after river restoration (increasing the leakage factor by a factor of 10 (d, e) and 100 (f)); (a) low river discharge (~5 m^3/s); (b,d) moderate flood (~40 m^3/s); (c, e, f) high flood (80–90 m^3/s). Each capture zone distribution is based on 10 aquifer realizations and describes the probability of a certain surface location belonging to the capture zone. The groundwater extraction at drinking water well 13 is constant at 0.046 m^3/s.

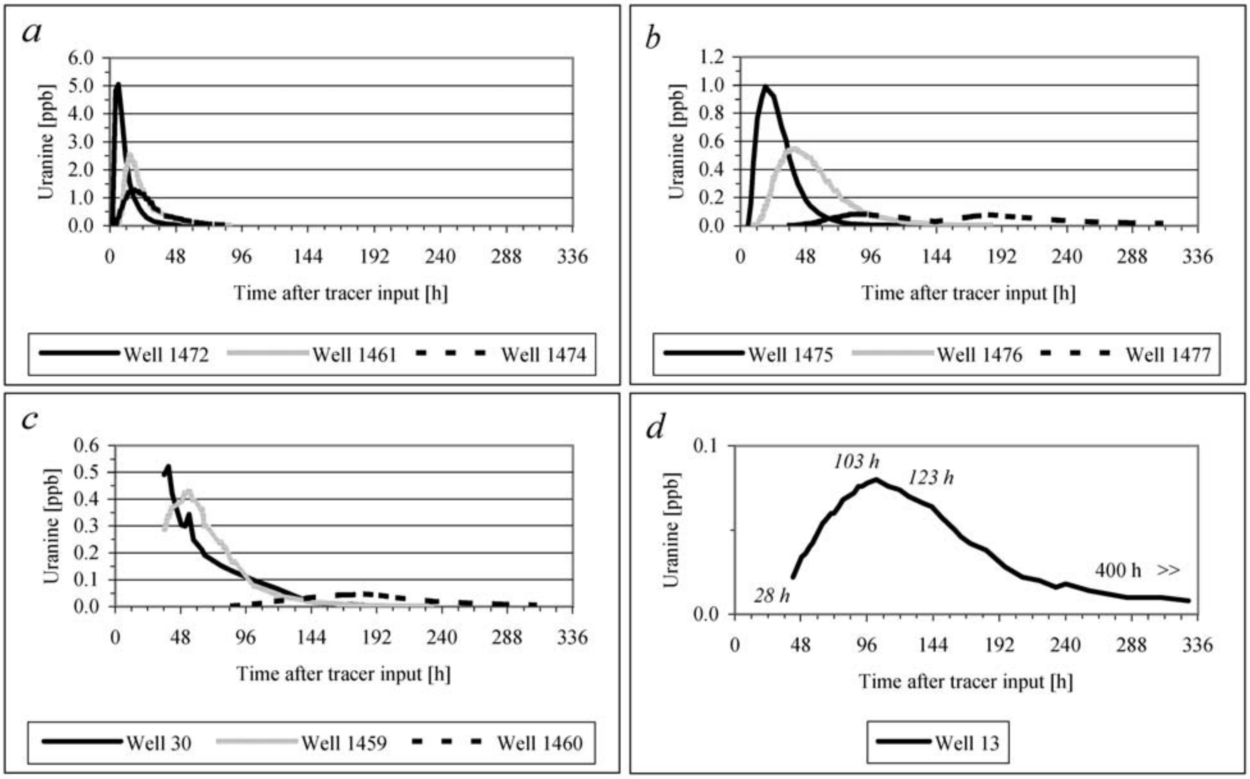

Figure 7. Breakthrough curves of Uranine in (a) monitoring wells 1472, 1461, 1474, located 12 meters from the river, (b) monitoring wells 1475, 1476, 1477, located 30 meters from the river, (c) monitoring wells 30, 1459, 1460, located 84 meters from the river, – samples were taken in the upper (1472, 1475, 30), middle (1461, 1476, 1459), and lower (1474, 1477, 1460) part of the aquifer, and (d) drinking water well 13, located 124 meters from the river, – samples were taken in the lower part of the aquifer. The moderate flood was 39.6 m^3/s. Note variable concentration scales in (a) – (d). See Figure 3 for well location information.

zone which amounts to approximately 5 l/s/(area), where the area represents this part of river section which is part of the well capture zone. It corresponds to approximately 10% of the extracted groundwater in drinking water well 13.

In comparison to the results from the large-scaled groundwater model (Fig. 5), the average groundwater residence time of 5.1 d – determined with the Uranine tracer experiment – supports the interpretation of a total mobilization of the riverbed as occuring under natural conditions during moderate to high river discharge or immediately after river restoration. However, the infiltration rate of river water of 5 l/s/(area) indicates no to moderate mobilization of the riverbed.

The river-groundwater transition zone is characterized by mixing of river water and groundwater and by changing groundwater residence times (Brunke and Gonser, 1997). Using the natural tracer Radon, the Radon water age can be determined. The theory and the limitations of this method are described by Hoehn and von Gunten (1989). Several authors have demonstrated the use of the dissolved Radon isotope Rn-222 for the determination of the average groundwater residence time (e.g., Hoehn, 2001; Dehnert et al., 1999; Hoehn and von Gunten, 1989). The cited authors assumed plug-flow conditions without mixing of river water and groundwater. The overall error attributed to uncertainties in sampling, measurement method, and counting statistics is estimated to be in the order of ±20% (Hoehn and von Gunten, 1989).

During the second Uranine tracer experiment, the groundwater as well as the river water was sampled for Rn-222. The Rn-222 activities are shown in Figure 8. The measurements in the river Wiese show low values during the experiment. The monitoring well 1472 near the river Wiese, which samples the upper part of the aquifer, shows a rapid increase in Rn-222 activity after the first smaller flood event on December 13, 1999, followed by a rapid decrease in Rn-222 activity at the beginning of the second larger flood event from December 18 to 21, 1999, and a renewed increase in Rn-222 activity at the end of the second flood event. The increase in Rn-222 activity after the first flood event is probably caused by the inclusion of zones with increased Rn-222 production such as iron hydroxide and manganese oxide precipitations on gravel surfaces. The decrease in Rn-222 activity may be caused by the dilution due to high infiltration of river water. Such biogeochemical changes in groundwater-infiltration sys-

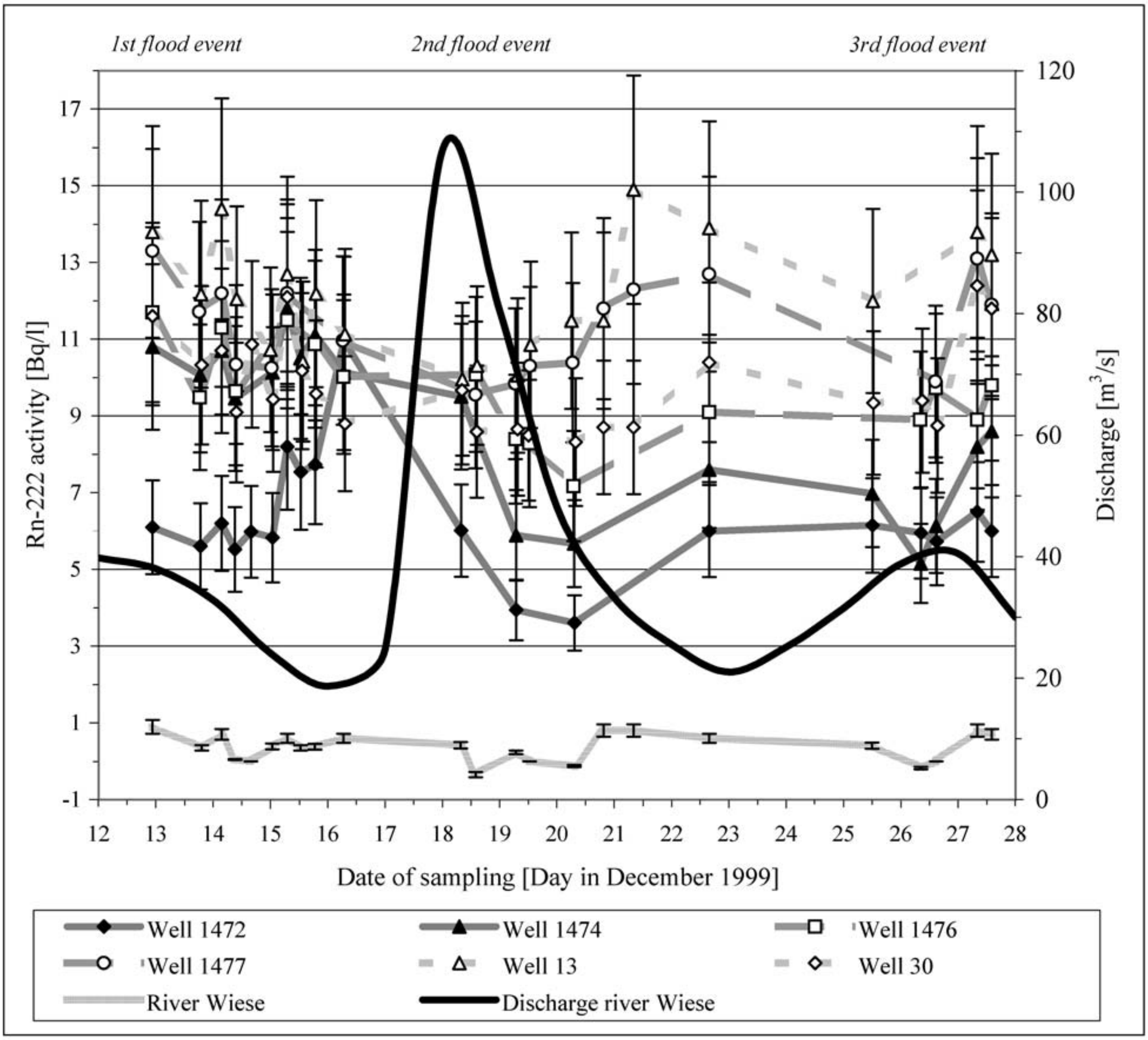

Figure 8. Activities of Rn-222 from December 13 to 28, 1999, in the river Wiese, monitoring wells 1472 and 1474, located 12 meters from the river, monitoring wells 1476 and 1477, located 30 meters from the river, monitoring well 30, located 70 meters from the river, and drinking water well 13 located 124 meters from the river. The error bars are ±20%.

tems are described for column experiments by von Gunten and Zobrist (1993) and for field experiments by von Gunten et al. (1991). The Rn-222 activity of well 1474 shows a similar shape, except for the initial increase of Rn-222 activity after the first flood event.

The Rn-222 activity of the monitoring wells 1476, 1477, and 30, and of drinking water well 13 varies between 7 and 15 Bq/l. The relative shape of the Rn-222 activity curves of these wells shows a decrease in Rn-222 activity after the first flood event and an increase in Rn-222 activity after the second flood event. However, the changes in Rn-222 activity are not significant, the values of the single wells vary within an error of ±20%. Therefore, these values do not allow further interpretation.

Assuming a steady-state Rn-222 activity of 19 Bq/l, measured in monitoring well 171 (Fig. 3a), the Radon water age for the extracted groundwater in drinking water well 13 is 4.2–7.5 days (101–180 h). Note that the average residence time for Uranine of 5.1 d falls within this range. Compared to the results from the groundwater models, the dominant time-to-peak and the average groundwater residence times could be accurately determined with Rn-222 measurements.

Physical and chemical data

The river-groundwater transition zone is characterized by microbiologically mediated redox processes such as aer-

Table 3. Data of physical and chemical parameters sampled in the river Wiese, the monitoring wells 1474, 1477, 1460, and drinking water well 13, before, during, and after river restoration; n.p.: below detection limit.

River restoration	Sampling state	Sampling location	Water temperature [°C]	pH [–]	Turbidity [FNU]	Oxygen saturation [% O2]	Dissolved organic carbon [mg C/l]	Electrical conductivity [µS/cm]	Chloride [mg Cl/l]	Hydrogencarbonate [mg HCO3/l]	Nitrate [mg NO3/l]	Nitrite [mg NO2/l]	Phosphate [mg PO4/l]	Sulfate [mg SO4/l]	Ammonium [mg NH4/l]	Calcium [mg Ca/l]
Before	Nov 09, 98	River Wiese	7.9	8.08	4.36	104	1.46	82	2.9	36	4.6	0.005	0.076	6.4	0.020	9.7
	Nov 09, 98	Well 1474	9.9	8.74	3.34	81	0.96	100	2.5	50	4.2	0.030	0.159	6.1	0.020	14.0
	Nov 09, 98	Well 1477	13.5	8.28	3.56	39	0.62	176	5.5	91	5.7	0.014	0.206	12.0	0.010	24.9
	Nov 09, 98	Well 1460	13.6	8.23	0.57	29	0.62	191	6.2	107	6.0	0.010	0.231	13.4	0.020	26.8
	Nov 09, 98	Well 13	13.4	8.05	0.07	67	0.68	183	3.9	98	5.5	n.p.	0.178	9.3	<0.009	27.6
	Dez 01, 98	River Wiese	4.2	7.90	1.44	101	1.08	135	9.0	53	6.0	0.016	0.091	10.3	0.030	26.8
	Dez 01, 98	Well 1474	6.5	8.58	3.95	89	0.70	136	6.7	59	5.8	0.010	0.159	10.1	<0.009	19.3
	Dez 01, 98	Well 1477	10.1	8.41	1.37	58	0.57	160	4.3	83	5.2	<0.01	0.235	9.6	n.p.	22.6
	Dez 01, 98	Well 1460	13.5	8.29	0.62	43	0.51	175	5.1	91	5.6	<0.01	0.250	11.3	n.p.	25.9
	Dez 01, 98	Well 13	12.8	8.10	0.05	76	0.52	170	4.2	91	5.6	n.p.	0.205	9.7	n.p.	26.8
	Jan 19, 99	River Wiese	4.9	7.87	2.11	101	1.36	116	6.6	49	5.3	0.024	0.062	9.0	0.052	14.2
	Jan 19, 99	Well 1474	5.6	8.61	2.37	83	0.76	134	9.0	58	5.8	n.p.	0.163	9.1	<0.009	18.5
	Jan 19, 99	Well 1477	5.6	8.53	1.05	83	0.59	140	6.5	68	5.6	n.p.	0.225	8.9	n.p.	20.3
	Jan 19, 99	Well 1460	11.6	8.40	0.29	80	0.49	150	5.9	77	5.6	n.p.	0.238	9.3	n.p.	22.1
	Jan 19, 99	Well 13	10.2	8.18	0.13	87	0.52	163	6.8	83	5.9	n.p.	0.178	9.3	n.p.	25.0
During	Feb 16, 99	River Wiese	1.8	7.94	1.20	101	1.17	122	7.6	51	5.8	0.035	0.098	10.2	0.089	14.9
	Feb 16, 99	Well 1474	3.6	8.57	3.32	95	0.82	138	8.2	62	6.2	n.p.	0.133	10.2	<0.009	19.5
	Feb 16, 99	Well 1477	6.5	8.60	6.47	89	0.82	136	8.2	63	5.8	n.p.	0.202	8.8	<0.009	20.3
	Feb 16, 99	Well 1460	7.9	8.49	0.13	91	0.63	143	7.8	68	5.9	n.p.	0.196	8.9	<0.009	20.5
	Feb 16, 99	Well 13	9.8	8.26	0.12	84	0.57	180	7.4	94	6.3	n.p.	0.181	10.7	<0.009	29.0
	Mrz 16, 99	River Wiese	6.2	7.78	1.80	102	1.02	75	4.8	29	3.9	0.006	0.034	5.3	0.031	7.9
	Mrz 16, 99	Well 1474	5.9	8.77	1.09	97	0.84	99	5.3	44	4.3	n.p.	0.165	5.9	<0.009	12.9
	Mrz 16, 99	Well 1477	5.9	8.62	0.20	106	0.67	136	9.2	58	5.8	n.p.	0.229	8.3	n.p.	18.5
	Mrz 16, 99	Well 1460	6.5	8.56	0.21	110	0.71	136	8.4	59	5.9	n.p.	0.241	8.1	n.p.	18.9
	Mrz 16, 99	Well 13	6.8	8.16	0.10	114	0.75	163	7.1	79	6.7	n.p.	0.166	9.2	n.p.	26.2
	Apr 20, 99	River Wiese	5.5	8.30	8.17	103	1.83	108	5.9	45	4.4	0.013	0.072	7.4	0.020	14.4
	Apr 20, 99	Well 1474	7.5	8.71	0.69	85	0.94	118	5.4	51	4.5	n.p.	0.167	7.4	<0.009	16.8
	Apr 20, 99	Well 1477	6.7	8.69	0.20	80	0.51	116	5.3	54	4.6	n.p.	0.282	6.8	<0.009	16.3
	Apr 20, 99	Well 1460	6.6	8.66	0.22	82	0.52	116	5.2	54	4.6	n.p.	0.294	6.7	<0.009	16.7
	Apr 20, 99	Well 13	7.7	8.23	0.13	86	0.49	170	6.0	82	6.1	n.p.	0.198	9.0	<0.009	26.5
After	Jun 22, 99	River Wiese	14.1	8.12	0.13	67	0.76	160	5.9	79	5.4	n.p.	0.163	11.4	n.p.	21.6
	Jun 22, 99	Well 1477	12.3	8.52	0.13	64	0.67	149	5.7	72	5.5	n.p.	0.247	11.0	n.p.	18.3
	Jun 22, 99	Well 1460	10.7	8.49	0.08	61	0.63	144	5.4	70	5.3	n.p.	0.254	10.2	0.010	18.9
	Jun 22, 99	Well 13	12.6	8.12	0.10	69	0.65	167	5.7	86	5.4	n.p.	0.192	11.1	n.p.	25.9
	Sep 21, 99	River Wiese	14.0	8.09	1.29	96	1.95	237	14.7	86	8.9	0.043	0.086	28.6	0.040	26.2
	Sep 21, 99	Well 1474	17.5	7.98	0.17	35	0.66	238	10.9	104	7.5	n.p.	0.083	23.8	0.240	32.4
	Sep 21, 99	Well 1477	16.3	8.24	0.16	33	0.52	217	9.7	96	7.4	n.p.	0.194	19.8	0.010	31.9
	Sep 21, 99	Well 1460	15.9	8.21	0.11	35	0.52	221	9.8	97	7.3	n.p.	0.193	20.1	n.p.	32.5
	Sep 21, 99	Well 13	16.0	7.89	0.07	54	0.52	252	9.8	118	7.1	n.p.	0.128	20.5	n.p.	39.2
	Dez 07, 99	River Wiese	3.9	8.00	3.65	94	1.34	102	5.5	41	5.2	<0.01	0.074	7.6	0.015	13.0
	Dez 07, 99	Well 1474	4.6	8.42	0.69	79	1.17	152	8.3	66	6.4	n.p.	0.167	9.1	<0.009	20.0
	Dez 07, 99	Well 1477	9.1	8.31	0.94	78	0.83	197	8.3	91	6.9	n.p.	0.207	14.8	<0.009	28.7
	Dez 07, 99	Well 1460	10.2	8.24	0.09	77	0.57	198	8.1	90	6.9	n.p.	0.231	14.7	<0.009	32.2
	Dez 07, 99	Well 13	11.9	8.19	0.10	81	0.51	315	7.6	103	6.8	n.p.	0.171	14.2	<0.009	31.6

obic respiration, denitrification, manganoxide reduction, etc. These riverbank-filtration processes are extensively described in von Gunten et al. (1991) and Sigg and Stumm (1996).

Water samples were taken in the river Wiese, in monitoring wells 1474, 1477, 1460, and in drinking water well 13 before, during, and after the river restoration of part 1 (18 different measurement times from November 1998 until December 1999). The water was analyzed for temperature, pH, turbidity, oxygen saturation, dissolved organic carbon, electrical conductivity, chloride, hydrogencarbonate, ammonium, nitrite, nitrate, phosphate, sulfate, and calcium. Table 3 shows some data before, during, and after river restoration.

The measured concentrations in the river Wiese are subject to large fluctuations and, due to the time delay of the signals, they cannot be directly correlated with the concurrently measured concentrations in the monitoring wells 1474, 1477, 1460, and in drinking water well 13. The data in Table 3 show that no significant changes in substance concentrations are noticeable before and after river restoration.

During the aerobic degradation of organic carbon, bacteria are using oxygen as a means for oxidization. The groundwater between the river Wiese and drinking water well 13 is mostly in an oxidizing condition. The carbon dioxide produced dissolves in the groundwater and reacts with the rock-forming minerals, e.g., carbonates and silicates. The weathering processes are responsible for the concentration of the main components calcium, magnesium, bicarbonate, sulfate, and silicic acid in the groundwater. Sodium, potassium, and chloride are probably controlled through these geochemical processes as well. The concentration of nitrate in the groundwater is primarily dependant on the mineralisation of organic nitrogen and secondarily on the nitrification of ammonium. The nitrate does not pose a public-health problem for the groundwater at this location. The phosphate concentration in the groundwater, however, is relatively high and may be attributed to agricultural use of fertilizers within the catchment area.

Additional biweekly temperature measurements show a clear horizontal layering of the groundwater, which remains virtually unchanged up to drinking water well 13 during the winter and summer months. Through the groundwater extraction a vertical mixing eventually takes place. The rather large temperature differences between winter and summer amount to 16 °C near the river Wiese and to 7 °C near the drinking water well 13. They support the modeling and tracer experiment results that a significant amount of groundwater recharge by the river Wiese occurs. The horizontal temperature distribution indicates the existence of preferential flow paths.

The physical and chemical data show that the chemical processes associated with infiltration of river water into the groundwater system predominantly occur in the hyporheic interstitial zone and in the riverbank within a range of a few meters up to a few 10 s of meters from the river.

Microbiological data

The microbiological data from the groundwater of drinking water well 13 in Figure 9 a–c document peak concentrations of microorganisms during flood events. The highest concentration in the river water is 3'000'000 cfu/ml (cfu: colony-forming unit) for heterotrophic plate counts, 10'600 cfu/100 ml for Escherichia coli, and 2'600 cfu/100 ml for Enterococcus. The concentration of microorganisms in drinking water well 13 increased during restoration activities (February 3 – June 8, 1999) and moderate flood events (river discharge >40 m^3/s) due to dredging and increase in permeability of the riverbed (179 cfu/ml for heterotrophic plate counts, 41 cfu/100 ml for Escherichia coli, 7 cfu/100 ml for Enterococcus). This represents a deterioration in groundwater quality. After completion of the river restoration, the concentration of microorganisms increased during flood events due to an increase in permeability of the riverbed (232 cfu/ml for heterotrophic plate counts, 11 cfu/100 ml for Escherichia coli, 7 cfu/100 ml for Enterococcus). However, for low and average river discharges, the concentration of microorganisms is comparable to that before river restoration. The delay of the flow peak in the river compared to the measured peak concentration of microorganisms in the drinking water well 13 amounts only to 1–2 days (24–48 h).

Figure 9 d–f shows average, minimum, and maximum concentrations of microorganisms along a hypothetical flow path between the river Wiese and drinking water well 13. The microorganisms predominantly occur in the hyporheic interstitial and within a few to a few 10 s of meters of the riverbank. A few microorganisms are able to reach drinking water well 13 by following the fast flow paths with larger and more pervious pores. The filtering effect along the fast flow paths is insufficient to retain these microorganisms.

The fast flow paths in the study site occur primarily in open-framework gravel (OW, OW/BM). The occurrence frequency and size of open-framework gravel deposits strongly determine the variance and the correlation length of the hydraulic conductivity. Transport experiments by Rehmann et al. (1999) show that the breakthrough of microorganisms is dependant on the variance of hydraulic conductivity within the aquifer. Thus, in heterogeneous systems the breakthrough of microorganisms occurs faster than that of conservative tracers. In the case of the Rhine and Wiese gravels, the hydraulic conductivity varies over four orders of magnitude (Jussel et al., 1994; Regli et al., 2002) and the

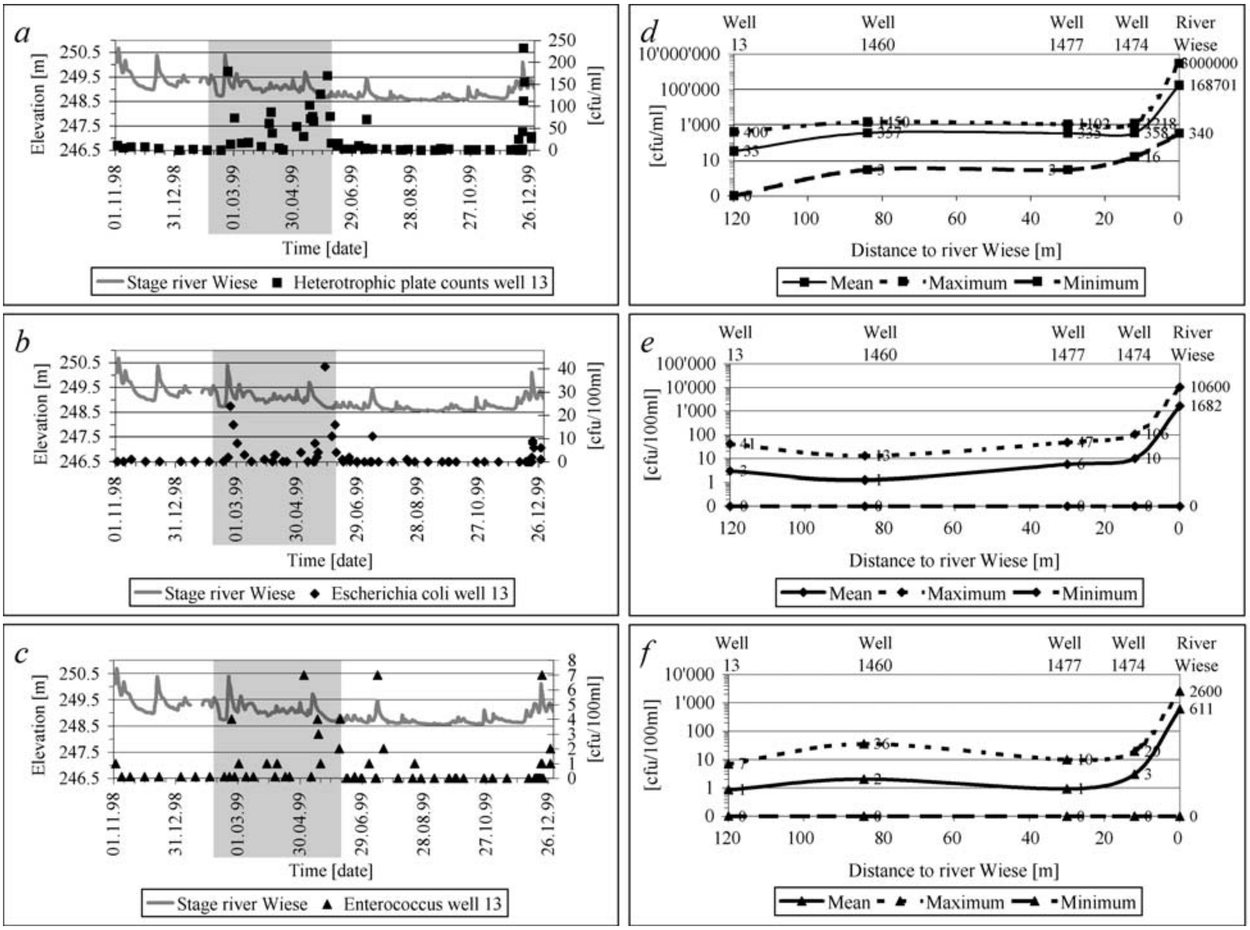

Figure 9. Concentrations of microorganisms measured in drinking water well 13 (left column) and along a hypothetical flow path – river Wiese, monitoring wells 1474, 1477, 1460, and drinking water well 13 – (right column) from November 1998 until December 1999: (a, d) Heterotrophic plate counts; (b, e) Escherichia coli; (c, f) Enterococcus. The groundwater extraction at drinking water well 13 amounts to 0.0 m^3/s in November 1998, 0.06 m^3/s from November 1998 until October 1999, and thereafter 0.046 m^3/s; cfu: colony-forming units; gray rectangel: time of restoration activities. Number of measurements (right column): 36 in river Wiese, 17 in monitoring well 1474, 19 in monitoring well 1477, 20 in monitoring well 1460, and 75 in drinking water well 13.

correlation length of the highly permeable structure type OW/BM is 36 m for Rhine gravel and 16 m for Wiese gravel (Table 2).

Observations at the study site confirmed the assumption that the reduction in concentration of microorganisms in the groundwater is dependant on the river discharge and the concentration of microorganisms in the river water, the filtering effect of the riverbed and the riverbank, the operation of drinking water well 13, the subsurface heterogeneitiy regarding permeability (filtering effect of the aquifer), and the biogeochemical conditions of the groundwater (Huggenberger, 2003).

Discussion and conclusions

The investigations demonstrate that well capture zones in the vicinity of infiltrating rivers might drastically change in size and orientation with respect to changing river infiltration, e. g., during high flow conditions. In order to accurately assess well capture zones, it is important to understand the boundary conditions and the influence of subsurface heterogeneity. In particular, the knowledge of highly permeable zones may help to define groundwater protection zones but also to define river sections where the structure of the riverbed and the riverbank can be restored to more natural conditions.

The use of stochastic methods is an effective and objective way to generate distributions of aquifer properties based on site-specific geological data of different quality. The integration of such distributions into groundwater flow and transport models is needed to determine well capture zones, taking into account data uncertainty. To manage the integration of hard and soft data into the stochastic simulation and visualization of the subsurface the software tool GEOSSAV (Regli et al., submitted) was used, which has been successfully tested and demonstrated with field experiments.

The results of the stochastic aquifer generation for the Lange Erlen study site include orientations of the sedimentary structure types representing the main flow directions of the river Rhine in the lower part of the aquifer and the tributary Wiese in the upper part of the aquifer. The spatial correlations of the sedimentary structure types of the Rhine gravel are horizontally around 20% and vertically around 45% larger than those of the Wiese gravel. In each aquifer realization, the initial probability density functions of the sedimentary structure types deviate less than ±10% from those which result in the probabilistic models.

The large-scaled, homogeneous groundwater model produced different possible well capture zones depending on changing boundary conditions (e.g., river discharge, riverbed structure). The runs with the small-scaled groundwater model show that the geometry of the well capture zone is strongly influenced not only by changing river discharge and riverbed structure, but also by subsurface heterogeneity. The stochastic approach in the small-scaled groundwater model does not lead to a clearly defined well capture zone, but to a plane representation of the probability of a certain surface location belonging to the capture zone, reflecting the uncertainty of the available data representing sedimentary structure types and the variability of their hydraulic conductivity and porosity values. This model takes into account the identified sedimentary structures and the statistical properties of the aquifer. As the number of aquifer realizations is relatively small, the results have a more qualitative character. However, they clearly illustrate the relative contribution of boundary fluxes and subsurface heterogeneity to changes in the well capture zone.

With the large-scaled, homogeneous groundwater model, the average groundwater residence time were determined and vary between 5 and 20 days depending on the boundary conditions. In comparison to the model results, the average groundwater residence time of 5.1 d (determined with the Uranine tracer experiment) is consistent with a flux boundary of an unclogged riverbed as occuring under natural conditions during moderate to high river discharge or immediately after river restoration. However, the corresponding river water infiltration at a rate of 5 l/s/(area) is more consistent with the model results when assuming no to moderate mobilization of the riverbed.

The physical and chemical data show that the chemical processes associated with infiltration of river water into the groundwater system predominantly occur in the hyporheic interstitial zone and in the riverbank within a range of a few meters up to a few 10 s of meters from the river. During the observation period of one year, significant changes in groundwater chemistry could not be detected.

The breakthrough of microorganisms during moderate and high flow conditions is dependant on the concentration of microorganisms in the river, the variance of the hydraulic conductivity within the aquifer, and the correlation length of the highly permeable structure types. The fast breakthrough occurrence of microorganisms and Uranine within 1–2 days in drinking water well 13 is in accordance with the sedimentological and geostatistical analysis of the aquifer.

The microbiological groundwater quality in the drinking water wells near the river Wiese is below drinking water standards during moderate and high flood events. Due to the frequency of flood events of about 10–12 times per year, it may not be possible to maintain operational security for groundwater extraction near the infiltrating river.

The concept of well capture zones as a planning instrument to prevent groundwater pollution in the vicinity of wells is not effective enough for drinking water wells with a significant amount of river water infiltration. Results from this study indicate that as long as the water quality in the river is not adequately controlled to avoid significant impacts on the operation of drinking water wells near the river, the concept of well capture zones proposed in Switzerland should be more rigorous. However, if these aspects are taken into account (e.g., operation of water supply according to river discharge and river water quality), it should be possible to perform river restorations within capture zones of wells which will still allow extracted groundwater to meet drinking water standards. As a consequence for conflicting situations in groundwater protection and river restoration, the understanding of the dynamics of the well capture zones at different flow conditions and the influence of subsurface heterogeneity between the river and the wells are basic requirements for a sustainable management of groundwater resources including the needs of river ecology.

Acknowledgments

We thank R. Wülser of the Industrial Services of the City of Basel for analyzing the chemical and microbiological parameters, M. Zehringer of the Cantonal Laboratory of Basel for providing the Rn-222 data, and numerous members of the Earth Sciences Department of the Basel University for their cooperation during the field experiments. We also thank W. Barrash and K. Bernet for reviewing and highly contributing to the manuscript. Special thanks to two anonymous reviewers for valuable critiques. Their comments have significantly improved the manuscript. This work is part of a Ph.D. thesis completed by Ch. Regli in 2002 at Basel University and was financially supported by the Swiss National Science Foundation, grant 20-56628.99.

References

Ayyub, B. M. and M. M. Gupta, 1997. Uncertainty Analysis in Engineering and Sciences: Fuzzy Logic, Statistics, and Neural Network Approach. Kluwer Academic, Dordrecht.

Brunke, M. and T. Gonser, 1997. The ecological significance of exchange processes between rivers and groundwater. Freshwater Biology **37**(1): 1–33.

Bundesamt für Wasser und Geologie (BWG), 2001. Hydrogeologisches Jahrbuch der Schweiz 2000.

Chiang, W.-H. and W. Kinzelbach, 2001. 3D-Groundwater Modeling with PMWIN. Springer, Heidelberg.

Dehnert, J., W. Nester, K. Freyer and H.-C. Treutler, 1999. Messung der Infiltrationsgeschwindigkeit von Oberflächengewässer mit Hilfe des natürlichen Isotops Radon-222. Grundwasser **1:** 18–30.

Deutsch, C. V. and A. G. Journel, 1998. GSLIB: Geostatistical Software Library and User's Guide, Second Edition, Applied Geostatistics Series. Oxford University Press, Oxford.

Environmental Modeling Systems Inc. (EMS-I), 2002. GMS: Groundwater Modeling System, EMS-I, South Jordan, Utah.

Gewässerschutzgesetz (GSchG, vom 24. Januar 1991, Stand 21. Dezember 1999), SR 814.20.

Gewässerschutzverordnung (GSchV, vom 28. Oktober 1998, Stand 18. Dezember 2001), SR 814.201.

Hoehn, E., 2001. Exchange processes between rivers and groundwaters – The hydrological and geochemical approach. Griebler, C. et al. (Eds.). Groundwater ecology: a tool for management of water resources. European Commission Environment and climate programme. 55–68.

Hoehn, E. and H. R. von Gunten, 1989. Radon in groundwater – a tool to assess infiltration from surface waters to aquifers. Water Resources Research **25**(8): 1795–1803.

Huggenberger, P., 2003. Transport von Mikroorganismen. In: Auckenthaler, A., Huggenberger, P. (Eds). Pathogene Mikroorganismen im Grund- und Trinkwasser, Transport – Nachweismethoden – Wassermanagement. Birkhäuser, Basel, 55–77.

Huggenberger, P. and Ch. Regli, 1998. Pilotprojekt Revitalisierung Wiese: Voruntersuchungen Grundwasser, Markierversuch Lange Erlen, Brunnen 8013. Tiefbauamt Basel-Stadt.

Jussel, P., F. Stauffer and T. Dracos, 1994. Transport modeling in heterogeneous aquifers: 1. statistical description and numerical generation of gravel deposits. Water Resources Research **30**(6): 1803–1817.

Kinzelbach, W., M. Marburger and W.-H. Chiang, 1992. Bestimmung von Brunneneinzugsgebieten in zwei und drei räumlichen Dimensionen. Geologisches Jahrbuch, Reihe C, Heft 61, Bundesanstalt für Geowissenschaften und Rohstoffe und Geologische Landesämter in der Bundesrepublick Deutschland, Hannover.

Kinzelbach, W. and R. Rausch, 1995. Grundwassermodellierung, Eine Einführung mit Übungen. Gebrüder Bornträger, Berlin.

Lerner, D. N., 1992. Well catchments and time-of-travel zones in aquifers with recharge. Water Resources Research **28**(10): 2621–2628.

Noack, T., 1993. Geologische Datenbank der Region Basel. Eclogae Geologicae Helveticae **86:** 283–301.

Noack, T., 1997. Geologische Datenbank der Region Basel – Konzept und Anwendungen. Mitteilungen der Schweizerischen Gesellschaft für Boden- und Felsmechanik **133:** 13–18.

Poeter, E. P. and S. A. McKenna, 1995. Reducing uncertainty associated with ground-water flow and transport predictions. Ground Water **33**(6): 899–904.

Rauber, M., F. Stauffer, P. Huggenberger and T. Dracos, 1998. A numerical three-dimensional conditioned/unconditioned stochastic facies type model applied to a remediation well system. Water Resources Research **34**(9): 2225–2233.

Regli, Ch., P. Huggenberger and M. Rauber, 2002. Interpretation of drill core and georadar data of coarse gravel deposits. Journal of Hydrology **255:** 234–252.

Regli, Ch., L. Rosenthaler and P. Huggenberger, GEOSSAV: a tool for the integration of hard and soft data into the stochastic simulation and visualization of the subsurface. Submitted to Computers & Geoscience, December, 2002.

Rehmann, L. L. C., C. Welty and R. W. Harvey, 1999. Stochastic analysis of virus transport in aquifers. Water Resources Research **35**(7): 1987–2006.

Reichert, P. and C. Pahl, 1999. Wie können Modelle zu Umweltentscheiden beitragen? EAWAG news **47d:** 3–5.

Rohrmeier, M., 2000. Geologische Modelle im Anströmbereich von Wasserfassungen. Diplomarbeit, Universität Basel.

Schudel, B., D. Biaggi, T. Dervey, R. Kozel, I. Müller, J. H. Ross and U. Schindler, 2002. Einsatz künstlicher Tracer in der Hydrogeologie – Praxishilfe. Bundesamt für Wasser und Geologie, Bern.

Siegenthaler, C. and P. Huggenberger, 1993. Pleistocene Rhine gravel: deposits of a braided river system with dominant pool preservation. In: Best, C.L., Bristow, C.S. (Eds.). Braided Rivers. Geological Society Special Publication **75:** 147–162.

Sigg, L. and W. Stumm, 1996. Aquatische Chemie: Eine Einführung in die Chemie wässeriger Lösungen und natürlicher Gewässer. vdf Hochschulverlag an der ETH Zürich.

van Leeuwen, M., Ch. B. M. te Stroet, A. P. Butler and J. A. Tompkins, 1998. Stochastic determination of well capture zones, Water Resources Research **34**(9): 2215–2223.

Vassolo, S., W. Kinzelbach and W. Schäfer, 1998. Determination of a well head protection zone by stochastic inverse modeling. Journal of Hydrology **206**(3–4): 268–280.

von Gunten, H. R., G. Karametaxas, U. Krähenbühl, M. Kuslys, R. Giovanoli, E. Hoehn and R. Keil, 1991. Seasonal biogeochemical cycles in riverborne groundwater. Geochimica et Cosmochimica Acta **55:** 3597–3609.

von Gunten, U. and J. Zobrist, 1993. Biogeochemical changes in groundwater-infiltration systems: column studies. Geochimica et Cosmochimica Acta **57:** 3895–3906.

Weissmann, G. S., S. F. Carle and G. E. Fogg, 1999. Three-dimensional hydrofacies modeling based on soil surveys and transition probability geostatistics. Water Resources Research **35** (6): 1761–1770.

Zechner, E., L. Hauber, Th. Noack, J. Trösch and R. Wülser, 1995. Validation of a groundwater model by simulating the transport of natural tracers and organic pollutants. In: Leibundgut, Ch. (Ed.). Tracer Technologies for Hydrological Systems. IAHS Publ. **229:** 57–64.